Four-component relativistic density-functional theory calculations of nuclear spin–rotation constants: Relativistic effects in p-block hydrides

Stanislav Komorovsky,[*] Michal Repisky, Elena Malkin, Taye B. Demissie, and Kenneth Ruud

Department of Chemistry, Centre for Theoretical and Computational Chemistry, UiT The Arctic University of Norway, Tromsø, Norway

E-mail: stanislav.komorovsky@uit.no

Abstract

We present an implementation of the nuclear spin–rotation (SR) constants based on the relativistic four-component Dirac–Coulomb Hamiltonian. This formalism has been implemented in the framework of Hartree–Fock and Kohn–Sham theory, allowing assessment of both pure and hybrid exchange–correlation functionals. In the density-functional theory (DFT) implementation of response equations, a non-collinear generalized gradient approximation (GGA) has been used. The present approach enforces a restricted kinetic balance condition for the small component basis at the integral level, leading to very efficient calculations of the property. We apply the methodology to study relativistic effects on the spin–rotation constants by performing calculations on XH_n ($n = 1$–4) for all elements X in the p–block of the periodic table, and comparing

[*]To whom correspondence should be addressed

the effects of relativity on the nuclear SR tensors to that observed for the nuclear magnetic shielding tensors. Correlation effects as described by density-functional theory are shown to be significant for the spin–rotation constants, whereas the differences between the use of GGA and hybrid density functionals are much smaller. Our calculated relativistic spin–rotation constants at the DFT level of theory are only in fair agreement with available experimental data. It is shown that the scaling of the relativistic effects for the spin–rotation constants (varying between $Z^{3.8}$ and $Z^{4.5}$) is as strong as for the chemical shieldings, but with a much smaller prefactor.

1 Introduction

Recently, Aucar *et al.*[1] presented a four-component relativistic theory for the nuclear spin–rotation constant arising from the interaction of the magnetic moment of a nucleus with the magnetic moment induced by the molecular rotation. The theory in ref 1 was considered in the laboratory coordinate system where the movement of the nuclei was added within the rigid rotor approximation. Xiao and Liu[2,3] later presented a more complete theory in body-fixed coordinates where also the vibrational motion of the nuclei was considered. The theory of Aucar *et al.*[1] assumed a non-relativistic motion for the nuclei and relativistic motion for the electrons. This approximation is well motivated since nuclei are much heavier and thus much slower than the electrons. However, when considering the formal expansion of the relativistic terms in $\frac{1}{c}$ instead of $\frac{v}{c}$ as dictated by the Lorenz factor in relativistic theory (here v is speed of the nuclei and c the speed of light), also Breit electron-nucleus terms should be considered as shown independently by Aucar *et al.*[4] and Xiao and Liu.[2] Indeed, this contribution was found to be negligible (less than 0.02% of the total spin–rotation constants in hydrogen halides)[5] as anticipated by Aucar *et al.*[1,4]

Malkin *et al.*[6] and Aucar *et al.*[4] presented the first molecular calculations of the spin–rotation constants at the relativistic four-component Dirac–Kohn–Sham and Dirac–Hartree–Fock levels of theory, respectively. Thereafter, numerous relativistic computational studies

of the spin–rotation constant have been presented, often with the focus on the consequence of using Flygare's relation[7–9] in determining the absolute shielding scale.[6,10–14] Although the Flygare relation is valid in the nonrelativistic case, special care must be taken when applying the relative relation between the paramagnetic contribution to the NMR shielding tensor and the electronic part of the spin–rotation tensor in the relativistic regime. As shown in our group,[6] the breakdown of the relation has significant consequences for the absolute shielding constant of ^{119}Sn, leading to errors of about 1000 ppm ($\sim 30\%$ of the absolute shielding) on a series of tetrahedral tin compounds. The observed discrepancy, which displays a surprisingly atomic nature, is a purely relativistic phenomenon arising from the differences in relativistic effects on the spin–rotation and NMR shielding tensors. Therefore, to better understand the phenomenon as well as to revise the absolute shielding scales and nuclear magnetic dipole moments of different elements, one needs to have consistent theoretical formulations and computationally feasible implementations of relativistic theories for both nuclear spin–rotation and NMR shielding tensors.

Recently, the evaluation of nuclear magnetic resonance parameters by means of relativistic density-functional theory has become a well-established task involving the use of restricted magnetically balanced (RMB) basis sets[15,16] for the small component wave function. The combination of the RMB concept with the gauge-including atomic orbitals (GIAO) ensures rapid basis set convergence of the NMR results towards the basis set limits.[17,18] Despite the complexity of the four-component formalism for the calculation of magnetic resonance parameters, modern implementations allow calculations on systems containing up to 100 atoms to be performed,[19–23] in particular if the two-electron integrals associated with the small component RMB basis are generated on-the-fly at the integral level.[24]

Stanton and Havriliak[25] showed that the origin of the variational collapse in the calculations based on the Dirac Hamiltonian when using uniform basis set are the off-diagonal terms in the kinetic part of the Hamiltonian. The elegant solution to this problem is the use of restricted kinetically balanced basis set (RKB) for the small component of the four-component

wave function.[25,26] In contrast to the external magnetic field appearing in the NMR shielding theory, the rotational momentum of the molecule does not yield any additional non-diagonal terms in the four-component Hamiltonian, which justifies the use of a simple RKB condition for the formulation and implementation of relativistic nuclear spin–rotation theory. Despite the simplification associated with the use of RKB instead of RMB basis, there are no implementations facilitating the use of hybrid exchange–correlation functionals for the evaluation of nuclear spin–rotation tensors in the four-component regime. The main goal of the present work is therefore to fill the apparent gap, taking into account the evidence that the use of hybrid functionals typically improve results of NMR properties of complex molecular systems.[27–30] In addition, we also present a new formulation of the non-collinear GGA kernels for the case of a time-reversal antisymmetric perturbation and systems with non-degenerate ground states. Finally, we apply this formalism to the study of the relativistic effects on the spin–rotation constants of the p–block hydrides, XH_n ($n = 1$–4), meant not only as an early assessment and benchmark of the implementation, but also allowing us to study the trends in the relativistic effects on the spin–rotation constants, in particular in comparison to the relativistic effects already well established for the NMR shielding tensors.[31,32]

The remainder of the paper is organized as follows: In Section 2, we describe the theory for the relativistic calculation of nuclear spin–rotation tensors within the density-functional and restricted kinetic balance framework. More precisely, Subsection 2.1 is devoted to the calculation of the perturbation-free density matrix, followed by the discussion of a one-electron spin–rotation Hamiltonian in Subsection 2.2, and finally in Subsection 2.3 we present working equations for the calculation of the linear response density matrix. In Section 3, we provide the computational details, and the analysis of the spin–rotation constants for p–block hydrides is presented and discussed in Section 4. Finally, we present some concluding remarks and an outlook in Section 5.

2 Theory and implementation

The nuclear spin–rotation tensor describes an interaction between the nuclear spin and the magnetic field generated by the rotating molecule.[9] The spin–rotation (SR) tensor can then be calculated as a bilinear derivative of the energy

$$C_{uv}^{\mathrm{N}} \equiv -\frac{d^2 E(\vec{I}^{\mathrm{N}}, \vec{L})}{dI_u^{\mathrm{N}} dL_v}\Bigg|_{\vec{I}^{\mathrm{N}}, \vec{L}=0} \tag{1}$$

where $\vec{I}^N$ denotes the nuclear spin of the N-th nucleus. In this work we consider non-degenerate electronic ground states, and the total angular momentum $\vec{L}$ is therefore represented solely by the rotational angular momentum of the molecule.

Compared to the previous implementations by Aucar *et al.*[4,5] and by Xiao *et al.*,[14,33] the present formalism utilizes the restricted kinetic balance condition for the small component basis, a non-collinear generalized gradient approximation (GGA) for the exchange–correlation response kernel, as well as the possibility to perform nuclear spin–rotation tensor calculations with hybrid density functionals. However, in contrast to the recent work by Xiao *et al.*,[33] we will not take advantage of rotational London orbitals to accelerate basis set convergence, but we believe that the basis sets used in this work are large enough to ensure near basis-set limit results. In the case when the basis set does not depend explicitly on the perturbation parameters, the SR tensor can be calculated from the expressions

$$C_{uv}^{\mathrm{N}} \equiv C_{uv}^{\mathrm{N,d}} + C_{uv}^{\mathrm{N,p}} \tag{2}$$

$$C_{uv}^{\mathrm{N,d}} = \mathrm{Tr}\left[\mathbf{h}^{\mathrm{N}(u,v)}\mathbf{D}^{(0,0)}\right] \tag{3}$$

$$C_{uv}^{\mathrm{N,p}} = \mathrm{Tr}\left[\mathbf{h}^{\mathrm{N}(u,0)}\mathbf{D}^{(0,v)}\right] \tag{4}$$

where $C_{uv}^{\mathrm{N,d}}$ and $C_{uv}^{\mathrm{N,p}}$ denote diamagnetic and paramagnetic (or electronic) contributions to the SR tensor, respectively. From now on, superscripts $(0,0)$, $\mathrm{N}(u,0)$, $(0,v)$ and $\mathrm{N}(u,v)$ will

refer to expansion coefficients in a Taylor series, such that the corresponding quantities read

$$\mathbf{D}^{(0,0)} \equiv \mathbf{D}|_{\vec{I}^{\mathrm{N}}, \vec{L}=0} \tag{5}$$

$$\mathbf{D}^{(0,v)} \equiv \left.\frac{\partial \mathbf{D}}{\partial L_v}\right|_{\vec{I}^{\mathrm{N}}, \vec{L}=0} \tag{6}$$

$$\mathbf{h}^{\mathrm{N}(u,0)} \equiv \left.\frac{\partial \mathbf{h}^{\mathrm{SR}}}{\partial I_u^{\mathrm{N}}}\right|_{\vec{I}^{\mathrm{N}}, \vec{L}=0} \tag{7}$$

$$\mathbf{h}^{\mathrm{N}(u,v)} \equiv \left.\frac{\partial^2 \mathbf{h}^{\mathrm{SR}}}{\partial I_u^{\mathrm{N}} \partial L_v}\right|_{\vec{I}^{\mathrm{N}}, \vec{L}=0} \tag{8}$$

Unless otherwise stated, the Hartree system of atomic units will be used throughout the paper.

2.1 Ground-state density matrix $\mathbf{D}^{(0,0)}$

In the modern algebraic formulation of relativistic Dirac–Hartree–Fock (DHF) or Dirac–Kohn–Sham (DKS) theory, the single-particle states (four-spinors) are expanded in a set of n basis functions $\{X_\mu\}_{\mu=1}^n$

$$\varphi_i = \sum_\mu^n X_\mu C_{\mu i} = \sum_\mu^n \begin{bmatrix} X_\mu^{\mathrm{L}} & 0 \\ 0 & X_\mu^{\mathrm{S,RKB}} \end{bmatrix} \begin{bmatrix} C_{\mu i}^{\mathrm{L}} \\ C_{\mu i}^{\mathrm{S}} \end{bmatrix} \tag{9}$$

To ensure that the finite basis set expansion suits the relativistic variational calculations, the single-particle states must be represented over two distinct sets of basis functions, $\{X\} = \{X^{\mathrm{L}}, X^{\mathrm{S}}\}$. Each of the so-called large component $\{X^{\mathrm{L}}\}$ and small component $\{X^{\mathrm{S,RKB}}\}$ sets consists of two-component basis functions, governed to lowest order in c^{-2} by the RKB relation

$$X_\mu^{\mathrm{S,RKB}} = \frac{1}{2c} \vec{\sigma} \cdot \vec{p} \, X_\mu^{\mathrm{L}} \tag{10}$$

where X_μ^L refers to a scalar Gaussian-type function, $\vec{p}$ is the momentum operator, and $\vec{\sigma}$ is the vector of three Pauli spin matrices

$$\sigma_1 \equiv \begin{pmatrix} 0 & 1 \\ 1 & 0 \end{pmatrix} \qquad \sigma_2 \equiv \begin{pmatrix} 0 & -i \\ i & 0 \end{pmatrix} \qquad \sigma_3 \equiv \begin{pmatrix} 1 & 0 \\ 0 & -1 \end{pmatrix} \tag{11}$$

The expansion coefficients associated with a single-particle state form a $4n$-dimensional vector over the field of complex numbers, $\mathbf{C}_i \in \mathbb{C}^{4n}$. Within the Lagrangian and density matrix formalisms, these expansion coefficients are obtained by minimizing the Dirac–Hartree–Fock ($\lambda = 1$) or Dirac–Kohn–Sham ($0 \leq \lambda < 1$) energy functional

$$E^{\text{DKS/DHF}} = \text{Tr} \left\{ \mathbf{h}^D \mathbf{D} \right\} + \frac{1}{2} \text{Tr} \left\{ \mathbf{G}[\lambda, \mathbf{D}] \mathbf{D} \right\} + E^{\text{xc}} \left[(1 - \lambda), \mathbf{D} \right] \tag{12}$$

subject to the orthonormality condition, $\mathbf{C}_i^\dagger \mathbf{S} \mathbf{C}_j = \delta_{ij}$, where $\mathbf{S}$ is the overlap matrix, $S_{\mu\nu} = \langle X_\mu | X_\nu \rangle$. The four-component single-particle ground-state density matrix for a N_e-electron molecular system is constructed from expansion coefficients associated with the N_e lowest positive-energy states

$$\mathbf{D} \equiv \sum_i^{N_e} \mathbf{C}_i \mathbf{C}_i^\dagger \tag{13}$$

In eq 12, $\mathbf{h}^D$ is the matrix representation of the one-electron Dirac Hamiltonian in the RKB basis

$$\mathbf{h}^D = \begin{bmatrix} \mathbf{V}^{\text{Ne}} & \mathbf{T} \\ \mathbf{T} & \mathbf{W}^{\text{Ne}} - \mathbf{T} \end{bmatrix} \tag{14}$$

where $\mathbf{T}$ is the non-relativistic kinetic energy matrix, and $\mathbf{V}^{\text{Ne}}$ and $\mathbf{W}^{\text{Ne}}$ are the nuclear–electron attraction matrices over the large component and small component basis, respectively. The two-electron interaction matrix $\mathbf{G}$, described in the present implementation by the instantaneous Coulomb electron–electron interaction, consists of the Coulomb ($\mathbf{J}$) and

7

the exchange ($\mathbf{K}$) terms

$$\mathbf{G}[\lambda] = \mathbf{J} - \lambda\mathbf{K} = \begin{bmatrix} \mathbf{J}^{\mathrm{LL}} & \mathbf{0}_{2\times 2} \\ \mathbf{0}_{2\times 2} & \mathbf{J}^{\mathrm{SS}} \end{bmatrix} - \lambda \begin{bmatrix} \mathbf{K}^{\mathrm{LL}} & \mathbf{K}^{\mathrm{LS}} \\ \mathbf{K}^{\mathrm{SL}} & \mathbf{K}^{\mathrm{SS}} \end{bmatrix} \tag{15}$$

The scalar coefficient λ weights the admixture of the exact-exchange contribution with the DFT exchange–correlation part (E^{xc}), giving rise to pure DHF ($\lambda = 1$), pure DKS ($\lambda = 0$), or hybrid schemes ($0 < \lambda < 1$). For a detailed discussion of eq 15, see for instance ref 34.

In the non-collinear framework, the GGA exchange-correlation energy is a functional of the electron density n, the length of the spin vector s, and their gradients $\vec{\nabla}n$, $\vec{\nabla}s$

$$s \equiv \sqrt{\rho_x^2 + \rho_y^2 + \rho_z^2} \qquad n \equiv \rho_0 \tag{16}$$

$$\vec{\rho} = \sum_i^{N_e} \varphi_i^\dagger \, \vec{\Sigma} \, \varphi_i = \mathrm{Tr}\left[\mathbf{X}^\dagger \vec{\Sigma} \mathbf{X} \mathbf{D}\right] \tag{17}$$

where $\vec{\Sigma}$ is the four-component spin operator

$$\vec{\Sigma} \equiv \begin{pmatrix} \vec{\sigma} & 0 \\ 0 & \vec{\sigma} \end{pmatrix} \tag{18}$$

Van Wüllen[35] presented the non-collinear theory for DFT potentials dependent on the electron density and the spin density. Later, Scalmani and Frisch[36] proposed a definition of the non-collinear theory including the gradient of the electron density and spin density. Until now the discussion in this subsection is valid for any time-reversal symmetry of the ground state wave function. However, in the absence of magnetic perturbations and systems with non-degenerate ground states, the spin density, its gradient as well as derivatives of the exchange–correlation energy density $\varepsilon^{\mathrm{xc}}$ with respect to s and $\vec{\nabla}s$, are zero. Then, the

exchange–correlation potential obeys the simple form

$$E^{\mathrm{xc}} = \int \varepsilon^{\mathrm{xc}}[\,n, \vec{\nabla}n,\, s, \vec{\nabla}s\,]\,\mathrm{dV} \tag{19}$$

$$V^{\mathrm{xc},0}_{\mu\nu} \equiv \frac{dE^{\mathrm{xc}}}{dD_{\mu\nu}} = \int \left(\frac{\partial \varepsilon^{\mathrm{xc}}}{\partial n} \Omega^0_{\mu\nu} + \frac{\partial \varepsilon^{\mathrm{xc}}}{\partial(\vec{\nabla}n)} \cdot \vec{\nabla}\Omega^0_{\mu\nu} \right) \mathrm{dV} \tag{20}$$

$$\Omega^0_{\mu\nu} \equiv \frac{\partial n}{\partial D_{\mu\nu}} \qquad \vec{\nabla}\Omega^0_{\mu\nu} \equiv \frac{\partial(\vec{\nabla}n)}{\partial D_{\mu\nu}} \tag{21}$$

2.2 Nuclear spin–rotation Hamiltonian

The relativistic theory for calculating the nuclear spin–rotation tensor C^{N}_{uv} was for the first time presented by Aucar and coworkers.[1] In this theory, the nuclei are treated within the rigid rotor approximation where the nuclear vibrational motion is neglected. The four-component one-electron Hamiltonian has then the form

$$h^{\mathrm{SR}}(\vec{L}, \vec{I}^{\mathrm{N}}) = (\beta - 1_{4\times4})c^2 + c\vec{\alpha} \cdot \vec{p} + V^{\mathrm{nuc}}(\vec{r}) \tag{22}$$

$$- \vec{J}_{\mathrm{e}} \bar{\bar{I}}^{-1} \vec{L} \tag{23}$$

$$+ \vec{\alpha} \cdot \vec{A}_{\vec{I}^{\mathrm{N}}}(\vec{r}) \tag{24}$$

$$- \frac{1}{c}\,\vec{v}_{\mathrm{N}} \cdot \vec{A}_{\vec{I}^{\mathrm{N}}}(\vec{r}) \tag{25}$$

$$- \frac{1}{c} \sum_{\mathrm{M}\neq\mathrm{N}} Z_{\mathrm{M}}(\vec{v}_{\mathrm{M}} - \vec{v}_{\mathrm{N}}) \cdot \vec{A}_{\vec{I}^{\mathrm{N}}}(\vec{R}_{\mathrm{M}}) \tag{26}$$

where c is the speed of light, Z_{M} and $\vec{R}_{\mathrm{M}}$ represent the nuclear charge and position of M'th nucleus, $\vec{p}$ is the electron momentum operator, $\bar{\bar{I}}$ is the nuclear inertia tensor with respect to the center of mass $\vec{R}_{\mathrm{CM}}$, and $V^{\mathrm{nuc}}(\vec{r})$ is the nuclear potential, respectively. The vector potential generated by the N'th nucleus $\vec{A}_{\vec{I}^{\mathrm{N}}}$ with gyromagnetic ratio γ_{N}, the velocity $\vec{v}_{\mathrm{N}}$ of nucleus N in the rigid rotor approximation, and the electronic total angular momentum

operator $\vec{J}_e$ can be written as

$$\vec{A}_{\vec{I}^N}(\vec{r}) = \gamma_N \frac{\vec{I}^N \times \vec{r}_N}{|\vec{r}_N|^3} \qquad \vec{r}_N \equiv \vec{r} - \vec{R}_N \tag{27}$$

$$\vec{v}_N = \bar{\bar{I}}^{-1} \vec{L} \times (\vec{R}_N - \vec{R}_{CM}) \tag{28}$$

$$\vec{J}_e = \left[(\vec{r} - \vec{R}_{CM}) \times \vec{p} \right] 1_{4\times 4} + \frac{1}{2} \vec{\Sigma} \tag{29}$$

The four-by-four matrices β and $\vec{\alpha}$ in the standard representation[37] have the form

$$\beta \equiv \begin{pmatrix} 1 & 0 \\ 0 & -1 \end{pmatrix} \qquad \vec{\alpha} \equiv \begin{pmatrix} 0 & \vec{\sigma} \\ \vec{\sigma} & 0 \end{pmatrix} \tag{30}$$

In the work of Aucar et al.,[1] the motion of the nuclei was considered to be much smaller than the speed of light, making it possible to treat the nuclei as non-relativistic particles, whereas the electrons were treated as relativistic particles. It was shown independently by Xiao and Liu[2] and Aucar et al.[4] that in order to have a consistent theory for the nuclear spin–rotation constants, when expanding the Hamiltonian in $\frac{1}{c}$, the electron–nucleus Breit interaction should be added to the SR Hamiltonian. It turns out that this contribution has negligible effect on the SR results (less then 0.02% of the total spin–rotation constants in hydrogen halides),[5] proving that the original assumption of using a non-relativistic description for the nuclei is an excellent approximation. For this reason we will here omit the electron–nucleus Breit interaction. Interestingly, Aucar and coworkers[5] showed that much more important than the electron–nucleus Breit interaction is the Gaunt contributions to the electron–electron interaction.

As already noted in the work of Aucar et al.,[1] the sum of the two contributions to the SR tensor, eqs 25 and 26, will vanish at the equilibrium geometry. To rationalize this statement,

it is useful to rewrite these contributions

$$\frac{1}{c}\,\vec{v}_{\mathrm{N}}\cdot\left[\sum_{\mathrm{M}\neq\mathrm{N}}Z_{\mathrm{M}}\vec{A}_{\vec{I}^{\mathrm{N}}}(\vec{R}_{\mathrm{M}})-\vec{A}_{\vec{I}^{\mathrm{N}}}(\vec{r})\right]= \tag{31}$$

$$=\frac{\gamma_{\mathrm{N}}}{c}\,\vec{v}_{\mathrm{N}}\cdot\left[\vec{I}^{\mathrm{N}}\times\left(\sum_{\mathrm{M}\neq\mathrm{N}}Z_{\mathrm{M}}\frac{(\vec{R}_{\mathrm{M}}-\vec{R}_{\mathrm{N}})}{|\vec{R}_{\mathrm{M}}-\vec{R}_{\mathrm{N}}|^{3}}-\frac{(\vec{r}-\vec{R}_{\mathrm{N}})}{|\vec{r}-\vec{R}_{\mathrm{N}}|^{3}}\right)\right] \tag{32}$$

$$\equiv\frac{\gamma_{\mathrm{N}}}{c}\,\vec{v}_{\mathrm{N}}\cdot\left[\vec{I}^{\mathrm{N}}\times\vec{E}(\vec{R}_{\mathrm{N}})\right] \tag{33}$$

where $\vec{E}(\vec{R}_{\mathrm{N}})$ is the total electric field operator at nucleus N. The term in eq 33 is bilinear in the nuclear spin and angular momentum and will therefore enter in the final expression for the SR tensor as a diamagnetic term. When noting that diamagnetic contributions are expressed in perturbation theory as inner products over perturbation-free wave functions, it is clear that eq 33 will vanish at the equilibrium geometry since $Z_{\mathrm{N}}\vec{E}(\vec{R}_{\mathrm{N}})$ is the operator of the total force acting on the nuclei. In this work, we have also performed geometry optimization at the four-component Dirac–Kohn–Sham level of theory, and therefore the term in eq 31 can be neglected when the same basis set and DFT functional are used in calculations of the spin–rotation tensor. On the other hand, for non-equilibrium geometries or inconsistent calculations involving different exchange–correlation functionals or basis sets, eq 31 gives a non-vanishing contribution that cannot be neglected.

2.3 Linear response density matrix $\mathbf{D}^{(0,v)}$

In the following, summation over repeated indices is assumed and the following index notation is employed: i, j denote occupied positive energy molecular orbitals (MOs), a unoccupied positive and negative energy MOs, p all MOs, μ, ν are used for basis function indices and Cartesian directions are indexed by u, v, k, l, m.

In four-component theories, special attention must be paid to the choice of basis sets. For the off-diagonal four-component operators it is crucial to properly balance the basis set for small component wave functions.[15,25] This is the case for the ground-state molecular

orbital optimization (see Section 2.1), as well as for the calculation of magnetic properties such as NMR shielding or spin–spin coupling tensors.[15–17] Since the linear response operator in eq 23 is block diagonal, there is no need to employ additional balance in the basis for the small component of the MOs, as in the case of off-diagonal magnetic field operator.[15,38] As a consequence, the linear response molecular orbitals can be expanded solely in the basis of the perturbation-free (ground-state) MOs

$$\varphi_i^{(0,v)} = \beta_{pi}^v \varphi_p^{(0,0)} \tag{34}$$

Since the MOs $\varphi_i(\vec{I}^{\mathrm{N}}, \vec{L})$ are orthonormal, the expansion coefficients β_{pi}^v satisfy the relation

$$(\beta_{ji}^v)^* + \beta_{ij}^v = 0 \tag{35}$$

Then, the linear response density matrix can be written as

$$D_{\mu\nu}^{(0,v)} = C_{\mu a}^{(0,0)} \beta_{ai}^v C_{\nu i}^{(0,0)*} + C_{\mu i}^{(0,0)} \beta_{ai}^{v*} C_{\nu a}^{(0,0)*} \tag{36}$$

Employing standard techniques from perturbation theory, the beta coefficients can be expressed as

$$\beta_{ai}^v = \frac{C_{\mu a}^{(0,0)*} \left(h_{\mu\nu}^{(0,v)} + V_{\mu\nu}^{(0,v)} \right) C_{\nu i}^{(0,0)}}{\varepsilon_i^{(0,0)} - \varepsilon_a^{(0,0)}} \tag{37}$$

where $h_{\mu\nu}^{(0,v)}$ are the matrix elements of the one-electron operator h^{SR} defined in Section 2.2 and $V_{\mu\nu}^{(0,v)}$ denotes the kernel of the two-electron contribution to the energy contracted with the linear response density matrix. Since the angular momentum $\vec{L}$ is a time-reversal antisymmetric perturbation, the linear response contribution to the electron density is zero, and thus the Coulomb term ($\mathbf{J}$) does not contribute to the kernel. The final matrix elements of the kernel can therefore be written as

$$V_{\mu\nu}^{(0,v)} \equiv V_{\mu\nu}^{\mathrm{xc},v} \left[(1 - \lambda), \mathbf{D}^{(0,v)} \right] - \lambda K_{\mu\nu} \left[\mathbf{D}^{(0,v)} \right] \tag{38}$$

where the Dirac–Hartree–Fock exchange contribution $K_{\mu\nu}$ was defined in Section 2.1. Finally, the non-collinear exchange-correlation kernel for a GGA functional (for the case of a non-degenerate ground state) has the form

$$
\begin{aligned}
V_{\mu\nu}^{\mathrm{xc},v} = \int \Bigg(& \left.\frac{\partial^2 \varepsilon^{\mathrm{xc}}}{\partial s^2}\right|_{\vec{L}=0} \rho_k^{(0,v)}\, \Omega_{\mu\nu}^k \\
& + \left.\frac{\partial^2 \varepsilon^{\mathrm{xc}}}{\partial s\,\partial(\nabla_l s)}\right|_{\vec{L}=0} \rho_k^{(0,v)}\, \nabla_l \Omega_{\mu\nu}^k \\
& + \left.\frac{\partial^2 \varepsilon^{\mathrm{xc}}}{\partial(\nabla_l s)\,\partial s}\right|_{\vec{L}=0} \frac{\nabla_l s^v}{s^v} \rho_k^{(0,v)}\, \Omega_{\mu\nu}^k \\
& + \left.\frac{\partial^2 \varepsilon^{\mathrm{xc}}}{\partial(\nabla_l s)\,\partial(\nabla_m s)}\right|_{\vec{L}=0} \frac{\nabla_l s^v}{s^v} \rho_k^{(0,v)}\, \nabla_m \Omega_{\mu\nu}^k \Bigg)\, \mathrm{d}V
\end{aligned}
\tag{39}
$$

where

$$
s^v \equiv \sqrt{\left(\rho_x^{(0,v)}\right)^2 + \left(\rho_y^{(0,v)}\right)^2 + \left(\rho_z^{(0,v)}\right)^2}
\tag{40}
$$

$$
\Omega_{\mu\nu}^k \equiv \frac{\partial \rho_k^{(0,0)}}{\partial D_{\mu\nu}} \qquad \nabla_l \Omega_{\mu\nu}^k \equiv \frac{\partial (\nabla_l \rho_k^{(0,0)})}{\partial D_{\mu\nu}}
\tag{41}
$$

Note that the density of a non-degenerate wave function in the case of time-antisymmetric perturbations satisfies the relations

$$
\rho_x^{(0,0)} = \rho_y^{(0,0)} = \rho_z^{(0,0)} = \rho_0^{(0,v)} = 0
\tag{42}
$$

Wang and Ziegler[39] have presented for the first time the formulation of the non-collinear kernel within the local density-functional approximation for open-shell systems as well as in the closed-shell limit. In this work we describe a new formulation for the non-collinear GGA exchange–correlation kernel for systems with non-degenerate ground states. The only other formulation of a non-collinear GGA exchange–correlation kernel was presented by Olejniczak *et al.*[40] in the framework of NMR shielding constants calculations and by Bast *et al.*[41] in the framework of time-dependent density-functional theory. The expressions in refs 40 and 41 can be obtained from eq 39 by assuming the directions of the response spin density vector

$\vec{\rho}^{(0,v)}$ and of any of its gradients $\nabla_k \vec{\rho}^{(0,v)}$ to be equal, making the formulation presented in refs 40 and 41 a special case of expression 39.

The non-collinear GGA exchange–correlation kernel (eq 39) can be used for any kind of time-reversal antisymmetric perturbations, such as external magnetic fields or magnetic fields generated by nuclei, and therefore the same expression for the kernel can be employed in relativistic theories for NMR shielding or spin-spin coupling calculations. Note that this formulation was already applied by some of present authors in their earlier works.[42,43] Moreover, the same expressions can also be used in any two-component relativistic theories including spin-orbit coupling variationally, with the density and spin density obtained from a two-component wave function instead of a four-component one.

The key point in the non-collinear DFT theory is the definition of the spin density. Since the spin density for a non-degenerate ground state is zero in the absence of the perturbation ($\vec{L} = 0$), we will define the orientation of the spin according to the response spin density $\vec{\rho}^{(0,v)}$. In one formulation of non-collinear theory, the collinear potential/kernel is at every point in space calculated in the coordinate system where the z axis is in the direction of the spin vector. The z component of the spin density $\rho_z^{(0,v)}$ and its gradient $\vec{\nabla}\rho_z^{(0,v)}$ is then substituted with the length of the spin density s^v and its gradient $\vec{\nabla}s^v$. As a final step, the collinear operator is transformed to the laboratory frame using the unitary transformations

$$
\begin{aligned}
V_{\mu\nu}^{\mathrm{xc},v} = U^\dagger[\vec{\rho}^{(0,v)}] \Bigg(& \left.\frac{\partial^2 \varepsilon^{\mathrm{xc}}}{\partial s^2}\right|_{\vec{L}=0} s^v\, \Omega_{\mu\nu}^z \\
& + \left.\frac{\partial^2 \varepsilon^{\mathrm{xc}}}{\partial s\partial(\nabla_k s)}\right|_{\vec{L}=0} s^v\, \nabla_k \Omega_{\mu\nu}^z \\
& + \left.\frac{\partial^2 \varepsilon^{\mathrm{xc}}}{\partial(\nabla_k s)\partial s}\right|_{\vec{L}=0} \nabla_k s^v\, \Omega_{\mu\nu}^z \\
& + \left.\frac{\partial^2 \varepsilon^{\mathrm{xc}}}{\partial(\nabla_k s)\partial(\nabla_l s)}\right|_{\vec{L}=0} \nabla_k s^v\, \nabla_l \Omega_{\mu\nu}^z \Bigg) U[\vec{\rho}^{(0,v)}]
\end{aligned}
\tag{43}
$$

After some tedious but straightforward derivations, eq 39 is recovered.

3 Computational details

All calculations have been performed using a development version of the four-component relativistic DFT program ReSpect.[44] The molecular geometries were optimized at the relativistic Dirac–Kohn–Sham level of theory employing the BP86 functional[45,46] and the uncontracted all-electron Dyall valence triple-ζ basis sets (denoted as dyall-vtz).[47–49] For all systems, convergence to 10^{-5} for the norm of the molecular gradient was achieved, with the exception of H_2Te and H_2Po, where a more loose threshold of 10^{-4} was used. The optimized geometries are listed in Table 1.

The spin–rotation constants were calculated with the Dirac–Hartree–Fock and Dirac–Kohn–Sham methods, in the latter case using the ordinary non-relativistic density functionals BP86[45,46] and B3LYP,[50–52] though some relativistic effects were included through the use of the relativistic electron density and spin densities. Integration of the exchange–correlation potential and kernel was done numerically on a molecular grid of ultrafine quality with an adaptive size in the angular part combined with a fixed number of radial grid points: H (50), 2p elements (60), 3p elements (70), 4p elements (80), 5p elements (90) and 6p elements (100). The exchange–correlation potential and kernel were calculated analytically by means of an automatic differentiation technique, as implemented in the XCFun library.[53] The spin–rotation and NMR shielding results were obtained with uncontracted all-electron Dyall's relativistic core-valence quadruple-ζ basis sets (denoted as dyall-cvqz).[47,49] The choice of the basis set is justified by our earlier study, where we showed that the basis set convergence is achieved at this level of basis set quality.[13] The small component basis of the restricted kinetically balanced type was used in the spin–rotation constant calculations, whereas the NMR shielding calculations required the use of a more elaborate restricted magnetically balanced concept.[15] Non-relativistic results are obtained using the same functionals and basis as in the relativistic calculations. In all spin–rotation calculations, the center of nuclear mass was chosen as the center of rotation of the molecule. For the purpose of a direct comparison with the spin–rotation results, the gauge origin was also placed at the center of nuclear mass

in the NMR shielding calculations. In the work of Xiao and Liu,[2] the authors also included the vibrational motion of the nuclei. Since the major focus of the current work is on the implementation of four-component relativistic calculations of spin–rotation constants, we neglected such corrections here. Finally, the nuclear g-factors used in all calculations are taken from ref 54 with the exception of $g(^{209}Po)$ and $g(^{210}At)$ for which no experimental data exist, and therefore a g-factor of 1.0 was chosen for these nuclei.

Before proceeding to the discussion of the results, let us first comment on different conventions used by experimentalists when choosing the axis system for the spin–rotation tensor. In order to compare our results with experimental values, we have followed the conventions used in the respective publications. The conventions are as follows: For the HX, H_2X, and the two XH_3 series, we have calculated the spin–rotation tensor $\mathbf{C}$ in the principal axes of the nuclear inertia tensor $\mathbf{I}$, and the diagonal elements of the spin–rotation tensor (C_{aa}, C_{bb}, C_{cc}) are considered. If the eigenvalues of $\mathbf{I}$ are degenerate, we take the average value of the respective diagonal components of $\mathbf{C}$ (if the two components of $\mathbf{C}$ are also equal, we emphasize it using the notation $C_{ii} = C_{jj}$). In the case of the HX series, this results in two components being degenerate and one component being identically zero for both tensors. For H_2X, there are no degenerate components, and for XH_3 two eigenvalues of the nuclear inertia tensor are degenerate. In the case of NH_3, Kukolich[55] published results for a specific orientation of the axes system. The z axis is the C_3 symmetry axis, the x and the y axes are parallel to the plane of the hydrogens, with the x axis in the plane spanned by the z axis and one of the N-H bonds, and the y axis perpendicular to that plane. The XH_4 series is a special case since all three eigenvalues of $\mathbf{I}$ are degenerate. In contrast to the other molecules, eigenvalues of the spin–rotation tensors have been reported.[56] The eigenvalues of the spin–rotation tensor on the heavy atom are all degenerate, whereas on the hydrogen atoms, two of the eigenvalues are identical. We label the degenerate components as $C_\perp$ and the third component as $C_\parallel$. The published isotropic C_{iso} and anisotropic C_{ani} values are then defined as $C_{iso} = (C_{aa} + C_{bb} + C_{cc})/3$ and $C_{ani} = C_\perp - C_\parallel$, respectively.

4 Results

We will first compare our results to experimental data for the individual groups, before we look in more detail on the scaling behavior of the relativistic corrections to the spin–rotation constants. Our results for the calculated spin–rotation constants together with available experimental data are collected in Tables 2–6.

Spin–rotation tensors of the group 17 hydrides are collected in Table 2 together with available experimental data. Four-component relativistic calculations have previously been presented for the group 17 hydrides both at the Hartree–Fock[4] and density-functional level of theory.[14] The spin–rotation constants of HCl was also recently studied at the *ab initio* level, including also relativistic corrections.[10]

There are several things to note from the data in Table 2. First, the correlation effect as described by DFT is quite sizeable, both for the heavy atom and for the hydrogen. Part of this effect is due to the fact that spin–orbit corrections contribute both to the heavy-atom and hydrogen spin–rotation constant and it would appear that triplet instabilities affect the quality of the results obtained with Hartree–Fock [four-component calculations with excluded spin-orbit (no-SO) interaction: $C_{DHF}^{no\text{-}SO}(^{210}At) = -867.89$; $C_{DHF}^{no\text{-}SO}(^{1}H) = 20.00$; $C_{BP86}^{no\text{-}SO}(^{210}At) = -957.13$ and $C_{BP86}^{no\text{-}SO}(^{1}H) = 20.98$].[57] In general, correlation effects amount to about 10-20% of the spin–rotation constants for the lighter hydrogen halides. The correlation effects increase the magnitude of the spin–rotation constants for the heavy elements. In contrast, for the hydrogen spin–rotation constants, correlation increases the magnitude of the spin–rotation constants for the lighter hydrogen halides, has almost no effect for hydrogen bromide, and reduces the magnitude for the two heaviest hydrogen halides.

Another noteworthy observation from Table 2 is that relativistic effects are almost negligible for the heavy-element spin–rotation constants, with the exception of hydrogen astatide. In contrast, relativistic effects are noticeable for the hydrogen spin–rotation constants, increasing from about 1.5% even for hydrogen fluoride, to more than 100% for hydrogen iodide and almost 400% in the case of hydrogen astatide. This is due to the predominance of spin–

orbit effects in determining the total relativistic correction, an effect that in general is more important for lighter elements close to heavy elements than for the properties of the heavy elements themselves.[58]

Turning our attention now to the hydrogen chalcogenides, our results together with available experimental data are collected in Table 3. We recently performed a highly accurate calculation of the spin–rotation and nuclear magnetic shielding constants of $H_2{}^{17}O$ and $H_2{}^{33}S$, showing that relativistic effects are important in order to derive accurate absolute shielding scales, and also that relativistic effects need to be taken into account when comparing accurate coupled-cluster results with experimental spin–rotation constants even for as light an element as ^{33}S.

The data in Table 3 shows many of the same trends as observed in the case of the hydrogen halides: Rather small relativistic corrections to the spin–rotation constants of the heavy nucleus, with only the heaviest members as exceptions; Sizeable relativistic corrections to the hydrogen spin–rotation constants, fairly large electron correlation effects as described by DFT and in general poor agreement with experimental data. Although zero-point vibrational corrections are non-negligible,[59] they are in general not sufficient to significantly improve the agreement between our DFT results and experimental data.

In Table 4 we have collected our results for the hydrides of the pnictogens together with available experimental data for ammonia and phosphine. It is interesting to observe that for ammonia, for the $C_{aa} = C_{bb}$ components of the nitrogen nucleus as well as for the $(C_{aa} + C_{bb})/2$ component of hydrogen, electron correlation effects as described by DFT are rather small, and this is also partly the case for phosphine. Interestingly, for these components, zero-point vibrational corrections are sizeable (about 1 kHz)[60] and much more significant than both electron correlation as well as relativistic effects. This contrasts with the C_{cc} component for nitrogen, where zero-point vibrational corrections are negligible. In terms of the importance of the relativistic corrections, the results follow the trends observed for the group 16 and 17 hydrides, although it would appear that the relativistic effects are

less strong for the hydrogen spin–rotation constant than observed further to the right in the periodic table.

These small changes in the importance of relativistic corrections for the hydrogen spin–rotation constants becomes further accentuated as we move to the hydrides of the carbon group (Table 5). Indeed, for the isotropic hydrogen spin–rotation constant, the relativistic corrections are negligible, whereas somewhat larger relativistic corrections are seen for the anisotropic spin–rotation constant (amounting to about 25% in the case of plumbane). Also for the heavy elements the relativistic effects are limited, being at most 50% in the case of plumbane, and less than 12% for the lighter hydrides of the carbon group.

For the hydrides of the boron group (Table 6), no experimental data are available, and we do therefore not discuss these results in any further detail here. The effects of relativity on the spin–rotation constants follow largely the trends observed for the hydrides of the pnictogens, with the notable exception that the $(C_{aa} + C_{bb})/2$ component of the hydrogen spin–rotation constant has a very significant relativistic effect, and in particular for the heaviest members with TlH_3 being an extreme case.

Overall, agreement with experiment is seen to be poor, with the DHF results in general being in better agreement with experiment than both the relativistic B3LYP and BP86 results. This is due to limitations in current exchange–correlation functionals for the description of magnetic properties. We have recently demonstrated that agreement of calculated spin–rotation constants using DFT level of theory with accurate coupled-cluster singles and doubles with perturbative triples [CCSD(T)] is poor for molecules such as water and hydrogen sulfide.[59] In contradiction to trends in the results for compounds containing only light elements the DFT give significantly better agreement with experiment for Stannane (see Table 5). Therefore to draw any definite conclusions one need to study larger set of experimental data including systems containing heavy elements.

Let us now turn to a more qualitative assessment of the relativistic effects on the spin–rotation, and in particular the scaling of the relativistic effects with the charge of the heavy

element in these p-block hydrides. In the left part of Figures 1–5, we present scaling of the relativistic contributions to the spin–rotation constants of the heavy atoms. As already noted in ref 1, the spin–rotation constants are less affected by relativistic effects than the NMR shielding constants. However, we see from Figures 1–4 this is due to a smaller prefactor rather than by a reduced scaling factor with respect to the nuclear charge of the heavy element. Interestingly, the scaling of the electronic contribution to the SR constants is in most cases a bit higher than for the paramagnetic contribution to the NMR shielding constants. The only exception to this rule is the H_2X series, where the prefactor is of the same order as for the shielding constant, but where instead the scaling is smaller for spin–rotation constants.

In the right part of Figures 1–4, we demonstrate the failure of the non-relativistic Flygare relation[9] between paramagnetic contribution to the NMR shielding constants and electronic contribution to the spin–rotation constants. Indeed, for the lighter elements, relativistic effects are negligible for both properties (except in the case of highly accurate calculations), whereas with increasing atomic number, the difference in relativistic correction in the two properties breaks this relation. As shown in ref 1, in perturbation theory both properties share some of the relativistic contributions, where all contributions to the SR tensor are present in the NMR shielding tensor. Therefore, the more profound relativistic effects for the NMR shielding tensor can be attributed to the additional atomic relativistic contributions otherwise missing in the spin–rotation tensor.

For the hydrogen halides, the nonsystematic effect of relativity on the heavy-element spin–rotation constants (see Figure 5) prevented fitting the scaling properties.

5   Summary and concluding remarks

We have presented an implementation of the nuclear spin–rotation constants at the relativistic four-component Dirac–Coulomb Hartree–Fock and Kohn–Sham density-functional levels of theory, using both pure and hybrid exchange–correlation functionals. In the DFT im-

plementation, a non-collinear generalized gradient approximation has been used. To ensure efficient evaluations of the spin–rotation constants, the restricted kinetic balance condition has been imposed at the integral level.

We have applied this new formalism to investigate the effects of relativity on the spin–rotation constants of both the hydrogen and the heavy atoms of the p-block hydrides. It is shown that relativistic corrections to the spin–rotation constants of the heavy elements are smaller than the corresponding relativistic corrections to the shielding constants in terms of the relative magnitude of the relativistic corrections. However, in terms of the scaling of the relativistic effects with nuclear charge of the heavy element, the scaling laws are comparable, with the spin–rotation constants showing a somewhat more rapidly increasing relativistic effects with an exponent of the scaling factor varying between $Z^{3.8}$ and $Z^{4.5}$, whereas the scaling of the paramagnetic contribution to the shielding constants varies between $Z^{3.3}$ and $Z^{4.1}$. The origin of the difference in the relativistic corrections thus largely arises from a much smaller prefactor for the spin–rotation constants than for the shielding constants.

In contrast, relativistic corrections to the hydrogen spin–rotation constants are as large as the relativistic corrections to the proton shieldings. These results are due to the fact that whereas the spin–rotation constant is largely dominated by the spin–orbit interactions both for the hydrogen and heavy atoms, there are additional, large relativistic atom-centered contributions to the shielding constants, giving much larger relative corrections to the shielding constants of heavy elements than is observed for the relativistic corrections to the heavy-element spin–rotation constants.

Accurate experimental spin–rotation constants can be determined from the hyperfine structure of rotational microwave spectra. The agreement between our relativistic four-component DFT results, using both GGAs and hybrid functionals, and accurate experimental data is in general poor. As electron correlation effects, as described by density-functional theory, are found to be fairly substantial, and four-component relativistic Hartree–Fock theory gives much better agreement with experiment, it is clear that current relativistic

exchange–correlation functionals are not accurate enough for the systematic study of spin–rotation constants. As a consequence, there is reason for concern regarding the accuracy of current exchange–correlation functionals also for DFT calculations of nuclear magnetic shielding constants, as previously noted,[60] giving support for the use of chemical shifts when comparing DFT calculations of shielding constants with experimental observations.[32,61]

Acknowledgment

References

(1) Aucar, I. A.; Gómez, S. S.; De Azúa, M. C. R.; Giribet, C. G. *J. Chem. Phys.* **2012**, *136*, 204119.

(2) Xiao, Y.; Liu, W. *J. Chem. Phys.* **2013**, *138*, 134104.

(3) Xiao, Y.; Liu, W. *J. Chem. Phys.* **2013**, *139*, 034113.

(4) Aucar, I. A.; Gómez, S. S.; Melo, J. I.; Giribet, C. C.; Ruiz De Azúa, M. C. *J. Chem. Phys.* **2013**, *138*, 134107.

(5) Aucar, I. A.; Gómez, S. S.; Giribet, C. G.; Ruiz De Azúa, M. C. *J. Chem. Phys.* **2013**, *139*, 094112.

(6) Malkin, E.; Komorovsky, S.; Repisky, M.; Demissie, T. B.; Ruud, K. *J. Phys. Chem. Lett.* **2013**, *4*, 459–463.

(7) Ramsey, N. F. *Phys. Rev.* **1950**, *78*, 699–703.

(8) Flygare, W. H. *J. Chem. Phys.* **1964**, *41*, 793–800.

(9) Flygare, W. H. *Chem. Rev.* **1974**, *74*, 653–687.

(10) Jaszuński, M.; Repisky, M.; Demissie, T. B.; Komorovsky, S.; Malkin, E.; Ruud, K.; Garbacz, P.; Jackowski, K.; Makulski, W. *J. Chem. Phys.* **2013**, *139*, 234302.

(11) Ruud, K.; Demissie, T. B.; Jaszuński, M. *J. Chem. Phys.* **2014**, *140*, 194308.

(12) Jaszuński, M.; Demissie, T. B.; Ruud, K. *J. Phys. Chem. A* **2014**, *118*, 9588–9595.

(13) Demissie, T. B.; Jaszuński, M.; Malkin, E.; Komorovský, S.; Ruud, K. *Mol. Phys.* **2014**, *DOI: http://dx.doi.org/10.1080/00268976.2014.993343*.

(14) Xiao, Y.; Zhang, Y.; Liu, W. *J. Chem. Theory Comp.* **2014**, *10*, 600–608.

(15) Komorovský, S.; Repiský, M.; Malkina, O. L.; Malkin, V. G.; Malkin Ondík, I.; Kaupp, M. *J. Chem. Phys.* **2008**, *128*, 104101.

(16) Repiský, M.; Komorovský, S.; Malkina, O. L.; Malkin, V. G. *Chem. Phys.* **2009**, *356*, 236–242.

(17) Komorovský, S.; Repiský, M.; Malkina, O. L.; Malkin, V. G. *J. Chem. Phys.* **2010**, *132*, 154101.

(18) Cheng, L.; Xiao, Y.; Liu, W. *J. Chem. Phys.* **2009**, *131*, 244113.

(19) Komorovsky, S.; Repisky, M.; Ruud, K.; Malkina, O. L.; Malkin, V. G. *J. Phys. Chem. A* **2013**, *117*, 14209.

(20) Kelley, M. S.; Shiozaki, T. *J. Chem. Phys.* **2013**, *138*, 204113.

(21) Demissie, T. B.; Repisky, M.; Liu, H.; Ruud, K.; Kozlowski, P. M. *J. Chem. Theory Comp.* **2014**, *10*, 2125.

(22) Hrdá, M.; Kulich, T.; Repisky, M.; Noga, J.; Malkina, O. L.; Malkin, V. G. *J. Comput. Chem.* **2014**, *35*, 1725–1737.

(23) Reynolds, R. D.; Shiozaki, T. *Phys. Chem. Chem. Phys.* **2014**, *DOI: http://dx.doi.org/10.1039/c4cp04027a*.

(24) Repisky, M. INTEREST 2.0, An integral program for relativistic quantum chemistry, 2013.

(25) Stanton, R. E.; Havriliak, S. *J. Chem. Phys.* **1984**, *81*, 1910–1918.

(26) Kutzelnigg, W. *Int. J. Quantum Chem.* **1984**, *25*, 107–129.

(27) Wiberg, K. B. *J. Comput. Chem.* **1999**, *20*, 1299–1303.

(28) Cheeseman, J. R.; Trucks, G. W.; Keith, T. A.; Frisch, M. J. *J. Chem. Phys.* **1996**, *104*, 5497–5509.

(29) Helgaker, T.; Watson, M.; Handy, N. C. *J. Chem. Phys.* **2000**, *113*, 9402–9409.

(30) Autschbach, J. *Principles and Applications of Density Functional Theory in Inorganic Chemistry I*; Structure and Bonding; Springer Berlin Heidelberg, 2004; Vol. 112; pp 1–48.

(31) Fukui, H.; Baba, T. *J. Chem. Phys.* **1998**, *108*, 3854–3862.

(32) Autschbach, J.; Zheng, S. In *Ann. Rep. NMR Spectrosc.*; Webb, G. A., Ed.; 2009; Vol. 67; pp 1–95.

(33) Xiao, Y.; Zhang, Y.; Liu, W. *J. Chem. Phys.* **2014**, *141*, 164110.

(34) Dyall, K. G.; Faegri Jr., K. *Introduction to Relativistic Quantum Chemistry*; Oxford University Press: New York, 2007; Chapter 15, pp 277–294.

(35) van Wüllen, C. *J. Comput. Chem.* **2002**, *23*, 779–785.

(36) Scalmani, G.; Frisch, M. J. *J. Chem. Theory Comp.* **2012**, *8*, 2193–2196.

(37) Dyall, K. G.; Faegri Jr., K. *Introduction to Relativistic Quantum Chemistry*; Oxford University Press: New York, 2007; Chapter 4, pp 35–53.

(38) Kutzelnigg, W. *Phys. Rev. A* **2003**, *67*, 032109.

(39) Wang, F.; Ziegler, T. *J. Chem. Phys.* **2004**, *121*, 12191–12196.

(40) Olejniczak, M.; Bast, R.; Saue, T.; Pecul, M. *J. Chem. Phys.* **2012**, *136*, 014108.

(41) Bast, R.; Jensen, H. J. A.; Saue, T. *Int. J. Quantum Chem.* **2009**, *109*, 2091–2112.

(42) Demissie, T. B.; Repisky, M.; Komorovsky, S.; Isaksson, J.; Svendsen, J. S.; Dodziuk, H.; Ruud, K. *J. Phys. Org. Chem.* **2013**, *26*, 679–687.

(43) Demissie, T. B.; Kostenko, N.; Komorovsky, S.; Repisky, M.; Isaksson, J.; Bayer, A.; Ruud, K. *J. Phys. Org. Chem.* **2015**, *accepted*.

(44) ReSpect, version 3.4.0 (2014) – Relativistic Spectroscopy DFT program of authors Komorovsky, S.; Repisky, M.; Malkin, V. G.; Malkina, O. L.; Kaupp, M.; Ruud, K., with contributions from Bast, R.; Ekström, U.; Kadek, M.; Knecht, S.; Konecny, L.; Malkin-Ondik, I.; Malkin, E. See www.respectprogram.org, (accessed June 30, 2015).

(45) Becke, A. D. *Phys. Rev. A* **1988**, *38*, 3098–3100.

(46) Perdew, J. P. *Phys. Rev. B* **1986**, *33*, 8822–8824.

(47) Dyall, K. G. unpublished.

(48) Dyall, K. G. *Theor. Chem. Acc.* **2002**, *108*, 335–340.

(49) Dyall, K. G. *Theor. Chem. Acc.* **2006**, *115*, 441–447.

(50) Becke, A. D. *J. Chem. Phys.* **1993**, *98*, 5648–5652.

(51) Lee, C.; Yang, W.; Parr, R. *Phys. Rev. B* **1988**, *37*, 785–789.

(52) Stephens, P. J.; Devlin, F. J.; Chabalowski, C. F.; Frisch, M. J. *J. Phys. Chem.* **1994**, *98*, 11623–11627.

(53) Ekström, U.; Visscher, L.; Bast, R.; Thorvaldsen, A. J.; Ruud, K. *J. Chem. Theory Comp.* **2010**, *6*, 1971–1980.

(54) Cohen, R. E.; Cvitas, T.; Frey, J. G.; Holmström, B.; Kuchitsu, K.; Marquardt, R.; Mills, I.; Pavese, F.; Quack, M.; Stohner, J.; Strauss, H. L.; Takami, M.; Thor, A. J. *Quantities, Units and Symbols in Physical Chemistry, IUPAC Green Book, 3rd Edition*; IUPAC & RSC Publishing: Cambridge, 2008; pp 1–250.

(55) Kukolich, S. G. *J. Am. Chem. Soc.* **1975**, *97*, 5704–5707.

(56) Anderson, C. H.; Ramsey, N. F. *Phys. Rev.* **1966**, *149*, 14–24.

(57) Helgaker, T.; Lutnæs, O. B.; Jaszuński, M. *J. Chem. Theory Comp.* **2007**, *3*, 86–94.

(58) Manninen, P.; Ruud, K.; Lantto, P.; Vaara, J. *J. Chem. Phys.* **2005**, *122*, 114107, Erratum *ibid.* **124** 149901 (2006).

(59) Komorovsky, S.; Repisky, M.; Malkin, E.; Ruud, K.; Gauss, J. *J. Chem. Phys.* **2015**, *142*, 091102.

(60) Teale, A. M.; Lutnæs, O. B.; Helgaker, T.; Tozer, D. J.; Gauss, J. *J. Chem. Phys.* **2013**, *138*, 024111.

(61) Helgaker, T.; Jaszuński, M.; Ruud, K. *Chem. Rev.* **1999**, *99*, 293–352.

(62) Bass, S. M.; DeLeon, R. L.; Muenter, J. S. *J. Chem. Phys.* **1987**, *86*, 4305–4312.

(63) Cazzoli, G.; Puzzarini, C. *J. Mol. Spectrosc.* **2004**, *226*, 161–168.

(64) Dijk, F. P. V.; Dymanus, A. *Chem. Phys. Lett.* **1969**, *4*, 170–172.

(65) Dijk, F. P. V.; Dymanus, A. *Chem. Phys. Lett.* **1968**, *2*, 235–236.

(66) Puzzarini, C.; Cazzoli, G.; Harding, M. E.; Vázquez, J.; Gauss, J. *J. Chem. Phys.* **2009**, *131*, 234304.

(67) Helgaker, T.; Gauss, J.; Cazzoli, G.; Puzzarini, C. *J. Chem. Phys.* **2013**, *139*, 244308.

(68) Cupp, R. E.; Kempf, R. A.; Gallagher, J. J. *Phys. Rev.* **1968**, *171*, 60–69.

(69) Davies, P. B.; Neumann, R. M.; Wofsy, S. C.; Klemperer, W. *J. Chem. Phys.* **1971**, *55*, 3564–3568.

(70) Ozier, I.; Vitkevich, J. A.; Ramsey, N. F. *Abstr., 27th Symp. Mol. Spectrosc. 1972.*

(71) Itano, W. M.; Ozier, I. *J. Chem. Phys.* **1980**, *72*, 3700–3711.

(72) Ozier, I.; Lee, S. S.; Ramsey, N. F. *J. Chem. Phys.* **1976**, *65*, 3985–3993.

(73) Jameson, C. J.; Jameson, A. K. *Chem. Phys. Lett.* **1988**, *149*, 300–305.

(74) Ozier, I.; Crapo, L. M.; Lee, S. S. *Phys. Rev.* **1968**, *172*, 63–82.

(75) Laaksonen, A.; Wasylishen, R. E. *J. Am. Chem. Soc.* **1995**, *117*, 392–400.

Table 1: Optimized geometries of the *p*-block hydrides using DKS/BP86/dyall-vtz level of theory.

Molecule	X	r(H-X) [Å]	$\angle$(H-X-H) [°]
HX ($C_{\infty v}$)	F	0.9313	
	Cl	1.2919	
	Br	1.4319	
	I	1.6315	
	At	1.7485	
H$_2$X (C_{2v})	O	0.9701	104.09
	S	1.3545	91.73
	Se	1.4782	90.28
	Te	1.6755	89.73
	Po	1.7801	89.05
XH$_3$ (C_{3v})	N	1.0218	106.28
	P	1.4327	92.49
	As	1.5324	91.01
	Sb	1.7260	90.65
	Bi	1.8047	90.20
XH$_4$ (T_d)	C	1.0952	
	Si	1.4929	
	Ge	1.5327	
	Sn	1.7168	
	Pb	1.7598	
XH$_3$ (D_{3h})	B	1.1973	
	Al	1.5939	
	Ga	1.5603	
	In	1.7355	
	Tl	1.7431	

Table 2: Calculated and experimental spin–rotation constants of HX series (X = F, Cl, Br, I, At) [in kHz].

Molecule	Nucleus	DHF[a]	DKS[b] B3LYP	DKS[b] BP86	Exp.[c]
HF	^{19}F	-336.52	-356.99	-360.23 (-360.69)	-307.65±0.02[d]
	^{1}H	62.71	69.74	71.87 (70.83)	71.10±0.02[d]
HCl	^{35}Cl	-56.93	-61.72	-60.74 (-60.73)	-54.00±0.15[e]
	^{1}H	39.78	41.52	41.76 (38.98)	42.32±0.70[e]
HBr	^{79}Br	-290.84	-336.46	-335.10 (-333.94)	-290.83±0.08[f]
	^{1}H	44.45	44.98	44.48 (31.76)	41.27±0.31[f]
HI	^{127}I	-331.99	-403.90	-403.06 (-402.09)	-351.1±0.3[g]
	^{1}H	61.30	56.65	54.43 (24.65)	49.22±0.22[g]
HAt	^{210}At	-7.31	-485.36	-535.71 (-594.00)	
	^{1}H	150.17	109.86	100.61 (21.07)	

[a] Four-component DHF calculations. [b] Four-component DKS calculations for different DFT potentials. Non-relativistic values are in parenthesis. [c] The signs of the experimental values are changed to be consistent with sign conventions used in this work. [d] Ref 62 [e] Ref 63 [f] Ref 64 [g] Ref 65

Table 3: Calculated and experimental spin–rotation constants of H_2X series (X = O, S, Se, Te, Po) [in kHz].

Molecule	Tensor element[a]	Nucleus[b]	DHF[c]	DKS[d]		Exp.[e]
				B3LYP	BP86	
H_2O	C_{aa}	^{17}O	29.34	31.79	31.98 (32.05)	28.477±0.088[f]
	C_{bb}	^{17}O	33.08	32.13	31.21 (31.10)	28.504±0.071[f]
	C_{cc}	^{17}O	20.56	21.99	21.99 (21.99)	18.382±0.047[f]
	C_{aa}	^{1}H	32.34	34.31	35.04 (34.74)	34.45±0.19[f]
	C_{bb}	^{1}H	29.31	30.78	31.16 (30.94)	31.03±0.19[f]
	C_{cc}	^{1}H	31.13	32.70	33.18 (33.03)	32.91±0.10[f]
H_2S	C_{iso}	^{33}S	-37.74	-39.50	-38.30 (-38.06)	-35.14±0.49[g]
	C_{aa}	^{33}S	-20.57	-24.27	-23.90 (-23.82)	-22.08±0.27[g]
	C_{bb}	^{33}S	-67.14	-66.63	-63.78 (-63.19)	-59.05±0.26[g]
	C_{cc}	^{33}S	-25.50	-27.59	-27.21 (-27.17)	-24.30±0.77[g]
	C_{iso}	^{1}H	16.06	16.35	16.40 (15.54)	16.06±0.01[h]
	C_{aa}	^{1}H	17.30	17.81	17.89 (17.17)	
	C_{bb}	^{1}H	14.17	14.46	14.53 (13.08)	
	C_{cc}	^{1}H	16.70	16.79	16.79 (16.37)	
H_2Se	C_{aa}	^{77}Se	-116.31	-149.16	-149.95 (-146.83)	
	C_{bb}	^{77}Se	-355.98	-369.79	-358.27 (-340.59)	
	C_{cc}	^{77}Se	-125.10	-142.37	-142.88 (-141.95)	
	C_{aa}	^{1}H	17.71	18.10	17.96 (14.02)	
	C_{bb}	^{1}H	19.79	18.78	18.28 (10.84)	
	C_{cc}	^{1}H	14.70	14.62	14.58 (12.95)	
H_2Te	C_{aa}	^{125}Te	276.99	367.21	372.12 (351.22)	
	C_{bb}	^{125}Te	1032.93	1089.56	1054.88 (923.97)	
	C_{cc}	^{125}Te	296.79	347.96	351.00 (352.45)	
	C_{aa}	^{1}H	21.53	20.96	20.44 (10.56)	
	C_{bb}	^{1}H	34.08	29.21	27.36 (7.69)	
	C_{cc}	^{1}H	12.56	12.21	12.19 (9.69)	
H_2Po	C_{aa}	^{209}Po	-1110.58	-1481.80	-1482.34 (-868.64)	
	C_{bb}	^{209}Po	213.48	-189.39	-259.99 (-332.01)	
	C_{cc}	^{209}Po	-147.78	-225.11	-229.15 (-316.25)	
	C_{aa}	^{1}H	105.70	72.22	64.90 (6.44)	
	C_{bb}	^{1}H	59.82	48.51	45.14 (9.12)	
	C_{cc}	^{1}H	0.03	4.55	5.35 (8.26)	

[a] $C_{iso} = (C_{aa} + C_{bb} + C_{cc})/3$ [b] ^{1}H SR constants results for H_2S are calculated using ^{32}S isotope. [c] Four-component DHF calculations. [d] Four-component DKS calculations for different DFT potentials. Non-relativistic values are in parenthesis. [e] The signs of the experimental values are changed to be consistent with sign conventions used in this work. [f] Ref 66 [g] Ref 67 [h] Average of values for two different rotational transitions[68]

Table 4: Calculated and experimental spin–rotation constants of XH_3 series (X = N, P, As, Sb, Bi) [in kHz].

Molecule	Tensor element	Nucleus[a]	DHF[b]	DKS[c] B3LYP	DKS[c] BP86	Exp.
NH_3	$C_{aa} = C_{bb}$	^{14}N	-7.61	-7.67	-7.48 (-7.46)	-6.764 ± 0.005[d]
	C_{cc}	^{14}N	-7.21	-8.00	-7.99 (-7.97)	-6.695 ± 0.005[d]
	$(C_{aa} + C_{bb})/2$	^1H	17.72	17.99	18.15 (18.09)	17.73 ± 0.02[d]
	C_{cc}	^1H	18.71	19.10	19.24 (19.21)	19.05 ± 0.02[d]
	C_{aa}	^1H	4.01	3.85	3.90 (3.90)	3.28 ± 0.03[d]
	C_{bb}	^1H	31.39	32.09	32.34 (32.23)	32.26 ± 0.03[d]
	C_{cc}	^1H	18.71	19.10	19.24 (19.21)	19.01 ± 0.03[d]
PH_3	$C_{aa} = C_{bb}$	^{31}P	-120.02	-125.64	-122.25 (-121.26)	-114.90 ± 0.13[e]
	C_{cc}	^{31}P	-117.43	-129.44	-128.75 (-128.02)	-116.38 ± 0.32[e]
	$(C_{aa} + C_{bb})/2$	^1H	7.99	7.94	7.96 (7.75)	8.01 ± 0.08[e]
	C_{cc}	^1H	7.53	7.51	7.53 (7.44)	7.69 ± 0.19[e]
AsH_3	$C_{aa} = C_{bb}$	^{75}As	-105.46	-116.17	-115.73 (-110.79)	
	C_{cc}	^{75}As	-107.69	-123.87	-125.22 (-120.57)	
	$(C_{aa} + C_{bb})/2$	^1H	7.76	7.56	7.52 (6.54)	
	C_{cc}	^1H	6.63	6.63	6.64 (6.16)	
SbH_3	$C_{aa} = C_{bb}$	^{121}Sb	-247.86	-271.66	-271.28 (-239.98)	
	C_{cc}	^{121}Sb	-228.72	-271.33	-276.89 (-249.47)	
	$(C_{aa} + C_{bb})/2$	^1H	7.51	6.96	6.90 (4.85)	
	C_{cc}	^1H	4.68	4.88	5.00 (4.39)	
BiH_3	$C_{aa} = C_{bb}$	^{209}Bi	-323.81	-388.54	-390.91 (-264.04)	
	C_{cc}	^{209}Bi	-309.36	-402.62	-415.14 (-274.65)	
	$(C_{aa} + C_{bb})/2$	^1H	10.57	8.47	8.44 (4.35)	
	C_{cc}	^1H	2.17	3.56	4.11 (3.90)	

[a] To compare calculated values with experimental data, SR components C_{aa}, C_{bb} and C_{cc} of NH_3 molecule are obtained as average of $^{14}NH_3$ and $^{15}NH_3$. [b] Four-component DHF calculations. [c] Four-component DKS calculations for different DFT potentials. Non-relativistic values are in parenthesis. [d] Ref 55 [e] Ref 69

Table 5: Calculated and experimental spin–rotation constants of XH_4 series (X = C, Si, Ge, Sn, Pb) [in kHz].

Molecule	Tensor element[a]	Nucleus	DHF[b]	DKS[c] B3LYP	DKS[c] BP86	Exp.
CH_4	$C_{aa} = C_{bb} = C_{cc}$	^{13}C	-16.64	-18.41	-18.28 (-18.25)	$\pm 15.94 \pm 2.37$[d]
	C_{iso}	^1H	10.56	10.57	10.61 (10.60)	10.372 ± 0.083[e]
						10.5 ± 0.5[f]
	C_{ani}	^1H	18.64	18.89	18.94 (18.93)	18.370 ± 0.023[e]
SiH_4	$C_{aa} = C_{bb} = C_{cc}$	^{29}Si	41.23	45.53	45.70 (45.41)	$\pm 40.6 \pm 5$[g]
						41.3 ± 1[g]
	C_{iso}	^1H	4.13	4.00	3.97 (3.96)	3.88 ± 0.23[h]
						3.6 ± 0.6[f]
	C_{ani}	^1H	10.74	10.73	10.72 (10.71)	9.0 ± 3.5[h]
GeH_4	$C_{aa} = C_{bb} = C_{cc}$	^{73}Ge	17.52	19.96	20.38 (19.56)	
	C_{iso}	^1H	4.22	4.08	4.06 (3.96)	3.62 ± 0.20[h]
						4.0 ± 0.3[f]
	C_{ani}	^1H	9.46	9.42	9.42 (9.28)	5.5 ± 5.0[h]
SnH_4	$C_{aa} = C_{bb} = C_{cc}$	^{119}Sn	289.37	331.00	339.70 (304.27)	358.4 ± 18.1[i]
						368.8 ± 18.6[j]
	C_{iso}	^1H	3.20	3.10	3.10 (3.03)	
	C_{ani}	^1H	7.18	7.21	7.24 (7.02)	
PbH_4	$C_{aa} = C_{bb} = C_{cc}$	^{207}Pb	-335.31	-402.60	-419.29 (-285.89)	
	C_{iso}	^1H	3.21	3.02	3.08 (3.04)	
	C_{ani}	^1H	8.65	8.48	8.46 (6.82)	

[a] $C_{iso} = (C_{aa} + C_{bb} + C_{cc})/3$; $C_{ani} = C_\perp - C_\parallel$ [b] Four-component DHF calculations. [c] Four-component DKS calculations for different DFT potentials. Non-relativistic values are in parenthesis. [d] Ref 70 [e] Ref 71 [f] Ref 72 [g] Ref 73 [h] Ref 74 [i] Ref 75 (143 K) [j] Ref 75 (171 K)

Table 6: Calculated and experimental spin–rotation constants of XH_3 series (X = B, Al, Ga, In, Tl) [in kHz].

Molecule	Tensor element	Nucleus	DHF[a]	DKS[b]	
				B3LYP	BP86
BH_3	$C_{aa} = C_{bb}$	^{11}B	-104.05	-123.50	-126.38 (-126.35)
	C_{cc}	^{11}B	-13.46	-15.03	-14.97 (-14.96)
	$(C_{aa} + C_{bb})/2$	^{1}H	-2.61	-4.76	-5.50 (-5.43)
	C_{cc}	^{1}H	10.80	10.84	10.89 (10.89)
AlH_3	$C_{aa} = C_{bb}$	^{27}Al	-99.88	-121.49	-125.69 (-125.38)
	C_{cc}	^{27}Al	-99.87	-41.90	-42.12 (-41.84)
	$(C_{aa} + C_{bb})/2$	^{1}H	2.65	1.87	1.57 (1.90)
	C_{cc}	^{1}H	4.68	4.53	4.49 (4.51)
GaH_3	$C_{aa} = C_{bb}$	^{69}Ga	-270.37	-358.70	-379.06 (-367.75)
	C_{cc}	^{69}Ga	-104.22	-119.40	-123.08 (-117.56)
	$(C_{aa} + C_{bb})/2$	^{1}H	0.28	-1.46	-1.89 (0.67)
	C_{cc}	^{1}H	5.38	5.21	5.18 (5.14)
InH_3	$C_{aa} = C_{bb}$	^{115}In	-334.49	-455.07	-482.36 (-442.07)
	C_{cc}	^{115}In	-149.23	-169.12	-174.27 (-153.73)
	$(C_{aa} + C_{bb})/2$	^{1}H	-3.32	-4.86	-5.09 (1.03)
	C_{cc}	^{1}H	4.26	4.10	4.06 (4.08)
TlH_3	$C_{aa} = C_{bb}$	^{205}Tl	-1497.15	-2698.40	-2994.72 (-2155.09)
	C_{cc}	^{205}Tl	-941.26	-1087.18	-1135.72 (-713.37)
	$(C_{aa} + C_{bb})/2$	^{1}H	-19.36	-20.61	-20.02 (0.88)
	C_{cc}	^{1}H	5.29	4.89	4.83 (4.57)

[a] Four-component DHF calculations. [b] Four-component DKS calculations for different DFT potentials. Non-relativistic values are in parenthesis.
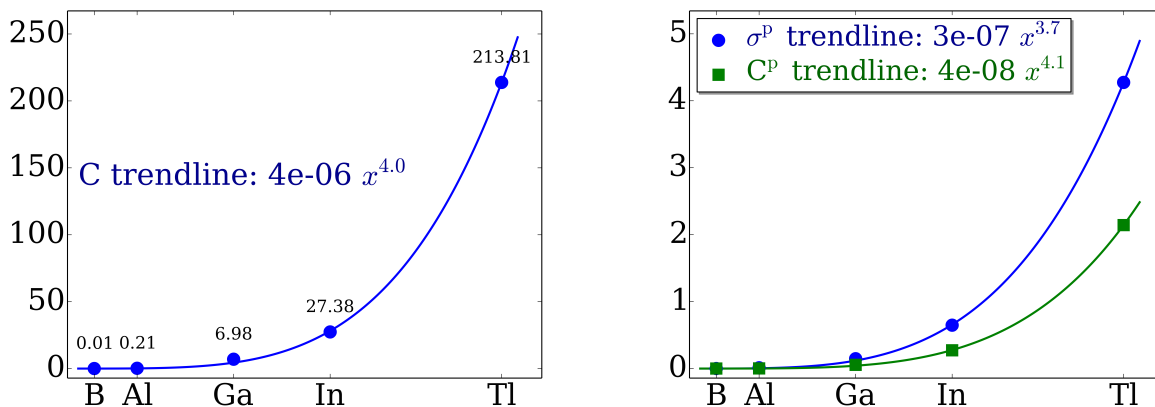
Figure 1: Relativistic contributions in XH_3 (X = B, Al, Ga, In, Tl) series as a function of atomic number. Left: the isotropic spin–rotation constant. Right: the paramagnetic part of isotropic NMR shielding (circle) and spin–rotation (square) constants in ppt.
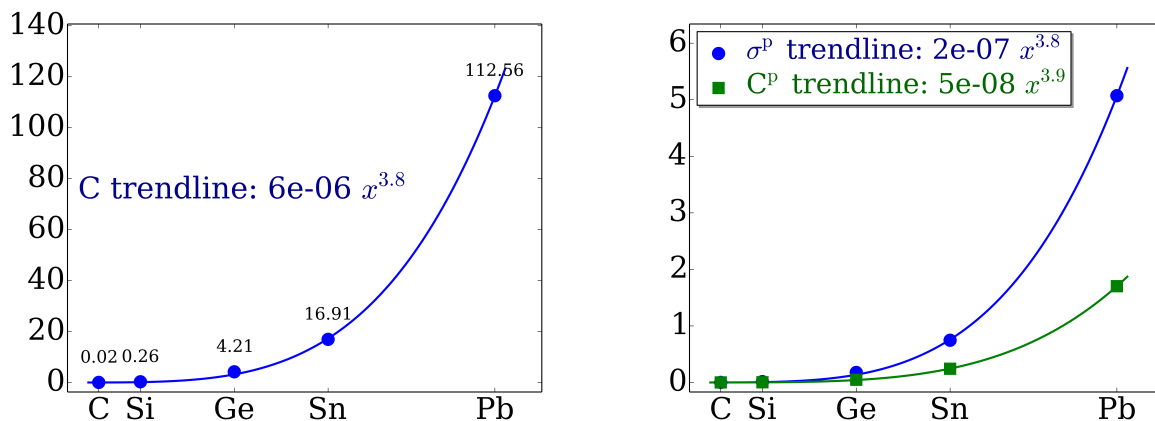

Figure 2: Relativistic contributions in XH_4 (X = C, Si, Ge, Sn, Pb) series as a function of atomic number. Left: the isotropic spin–rotation constant in kHz. Right: the paramagnetic part of isotropic NMR shielding (circle) and spin–rotation (square) constants in ppt.
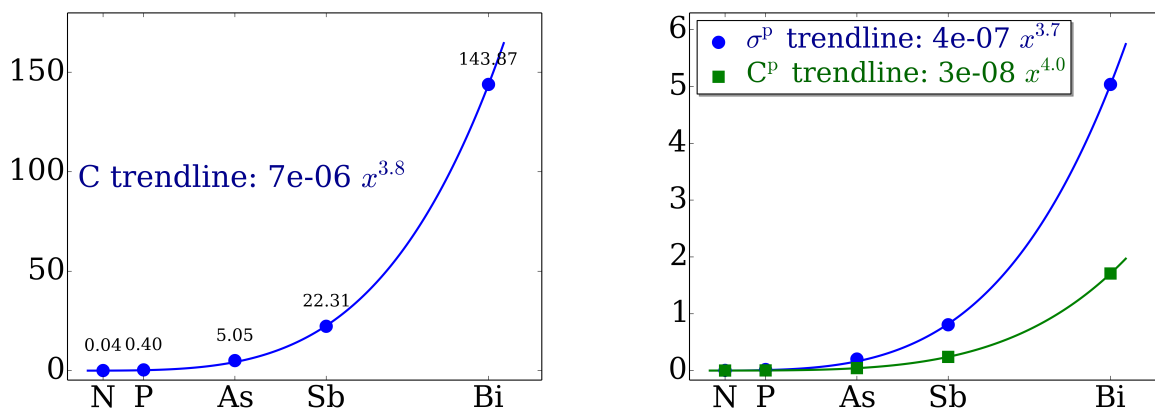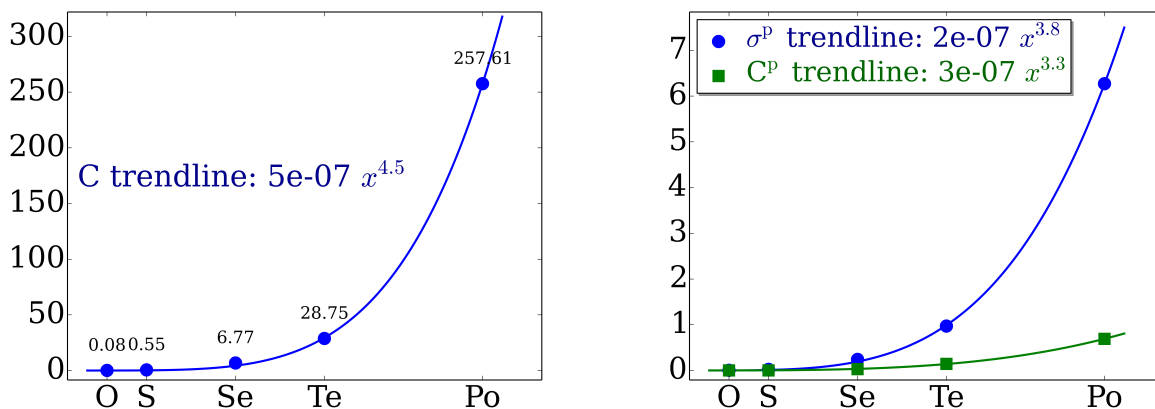
Figure 3: Relativistic contributions in XH_3 (X = N, P, As, Sb, Bi) series as a function of atomic number. Left: the isotropic spin–rotation constant in kHz. Right: the paramagnetic part of isotropic NMR shielding (circle) and spin–rotation (square) constants in ppt.

Figure 4: Relativistic contributions in H_2X (X = O, S, Se, Te, Po) series as a function of atomic number. Left: the isotropic spin–rotation constant in kHz. Right: the paramagnetic part of isotropic NMR shielding (circle) and spin–rotation (square) constants in ppt.
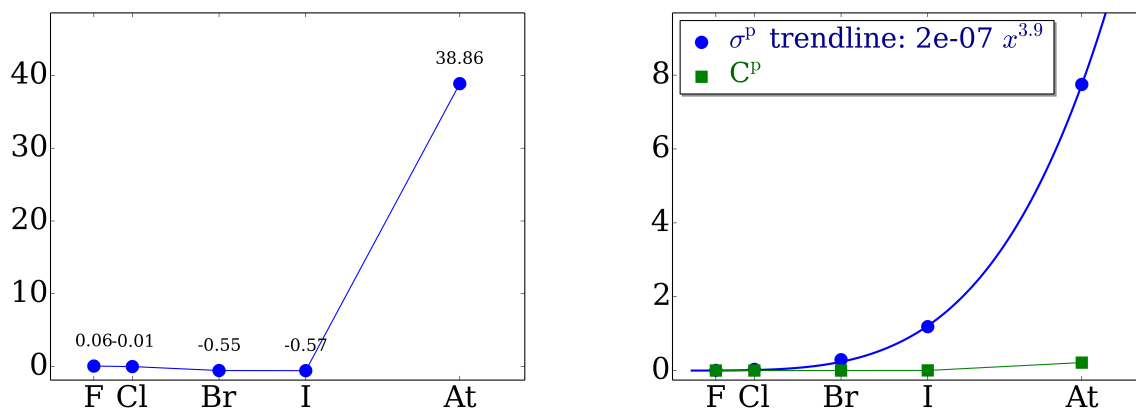
Figure 5: Relativistic contributions in HX (X = F, Cl, Br, I, At) series as a function of atomic number. Left: the isotropic spin–rotation constant in kHz. Right: the paramagnetic part of isotropic NMR shielding (circle) and spin–rotation (square) constants in ppt.

for Table of Contents use only

Four-component relativistic density-functional theory calculations of nuclear spin–rotation constants: Relativistic effects in p-block hydrides

Stanislav Komorovsky, Michal Repisky, Elena Malkin, Taye B. Demissie, Kenneth Ruud